2013 IEEE 10th International Symposium on Biomedical Imaging:
From Nano to Macro
San Francisco, CA, USA, April 7-11, 2013

SPLINE-BASED REFINEMENT OF VESSEL CONTOURS IN FUNDUS RETINAL IMAGES FOR WIDTH ESTIMATION

Alessandro Cavinato[⋆†] *Lucia Ballerini*[⋆⋆] *Emanuele Trucco*[⋆⋆] *Enrico Grisan*[†]

[⋆]School of Computing, University of Dundee, UK
[†]Department of Information Engineering, University of Padova, Italy

ABSTRACT

This paper presents a novel algorithm for refining the vessel contours obtained from retinal binary vessel maps. The refinement improves vessel width estimation. Our approach is based on fitting the two contours of each vessel in the binary map with a cubic spline curve, introducing a parallelism constraint between the two splines. The algorithm, evaluated on the REVIEW database, has a comparable accuracy to that of specialized, sophisticated width estimation algorithms.

Index Terms— Retinal images, vessel width, spline interpolation

1. INTRODUCTION

The analysis of retinal images plays a significant role in the clinical diagnosis of several pathologies; for instance, arteriosclerosis, hypertension and diabetes. Obtaining a binary vessel map from retinal images proves to be useful for many different purposes: among others, the measurement of vessel calibre as a biomarker for cardiovascular diseases. In recent years, many vessel segmentation algorithms were presented [1–4]. These methods aim to obtain a binary image identifying pixels belonging or not to the vascular structure. However, the problem of how to reliably estimate the vessel caliber is not addressed: in fact, width estimates taken from raw binary vessel maps, even in locations close to each other, present a relatively high standard deviation, due to the jagged vessel borders occurring in binary maps. Algorithms to estimate vessel diameter have been proposed in the literature [5]. Active contours are used in the Extraction of Segment Profiles (ESP) algorithm [6]. An alternative graph-based approach has recently been described [7]. Fiorin et al. [8] improved regularity of vessel borders by mean of spline interpolation.

This paper describes a novel algorithm for smoothing raw vessel contours in binary retinal vessels masks. For each processed vessel, after identifying its spline-smoothed centreline, the algorithm finds two cubic spline curves fitting the jagged contours. The coefficients of these splines are computed by solving an overconstrained system including both standard spline formulae and a parallel-tangent constraint. This constraint is very well suited for retinal vessels, because it ensures that the vessel profile is as similar as possible to a 2-D curvilinear pipe with parallel borders. The algorithm performs effectively on both linear and curved vessels.

Our algorithm does not aim to improve vessel detection but to improve the accuracy of width estimation from binary maps obtained from vessel detection algorithms. This is normally done by complex algorithms [6, 7] independent of vessel detection. Instead, we show that a new constrained spline fitting algorithm is sufficient to achieve results comparable to those of more sophisticated algorithms in tests on the standard dataset, REVIEW, for width estimation.

2. METHODOLOGY

2.1. Preprocessing

The vessel segmentation algorithm convolves the image with a Gaussian sliding window in order to enhance the contrast between vessel and non-vessel pixels, then applies a threshold to the response image [9]. This generates the binary vessel maps which are regularized by the proposed method.

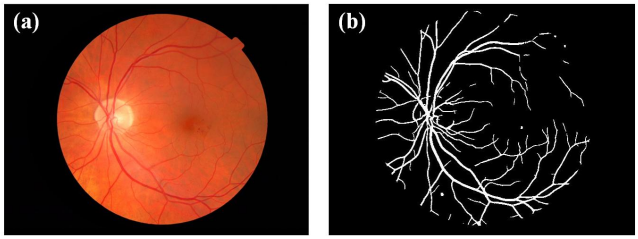

Fig. 1. Result of a segmentation procedure. (a) Original image of size 2240×1488 pixels. (b) Segmented binary image.

2.2. Vessel centreline computation and refinement

A first, rough set of centrelines can be easily obtained from a vessel binary map using a morphological thinning algorithm. The resulting image is a binary mask of the *vessel skeleton*. This binary structure can be divided in individual vessel segments by removing branching points. These points are detected by scanning the 8-neighbours of each skeleton pixel and removing pixels that have more than 2 neighbours lying on the skeleton. Segments shorter than 15 pixels are removed. Before proceeding with centreline refinement, a first estimate

⋆Research partially supported by Leverhume trust grant RPG-419

of vessel width can be computed using the distance transform of the binary vessel mask. To fit a natural cubic spline to the thinned vessel centreline, we transform the reference frame into the principal directions of the vessel points. This guarantees that the centreline of vessel segments between junctions is well represented as a function mapping each x value to a single y value. Centreline coordinates in the new reference frame are obtained. A natural cubic spline is then fitted to these points (subsampled every 10 pixels), obtaining a smooth centreline of the selected vessel.

Fig. 2. Vessel centreline refinement process. (a) Vessels from the binary mask. (b) Thinned centrelines. (c) Refined centrelines plotted on the binary vessel mask.

2.3. Vessel edge extraction

For each centreline pixel, C_j, we compute a segment d_j, normal to the centreline. To ensure that segment d_j will be long enough to pass even through the widest vessels, its length is set to w_j, where w_j is the preliminary vessel width at C_j, estimated from the distance transform described above. The image pixel intensity profile along d_j is computed using linear interpolation. Vessel edge points are detected as the two maxima of the first derivative of the interpolated intensity profile.

For each d_j, $j = 1, \ldots, m$, where m is the pixel length of the considered centreline, $2m$ coupled contour points, $\boldsymbol{q}_{A,j}$ and $\boldsymbol{q}_{B,j}$, are found and arranged in two lists, $Q_A = \{\boldsymbol{q}_{A,1}, \boldsymbol{q}_{A,2}, \ldots, \boldsymbol{q}_{A,m}\}$ and $Q_B = \{\boldsymbol{q}_{B,1}, \boldsymbol{q}_{B,2}, \ldots, \boldsymbol{q}_{B,m}\}$.

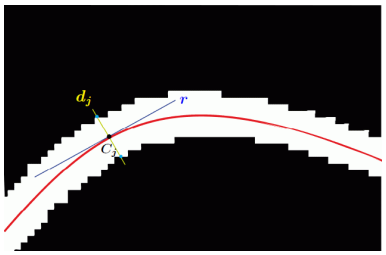

Fig. 3. Vessel edge points detection along d_j.

2.4. Contour refinement using coupled splines

Assuming that retinal vessel boundaries run approximately aligned, a parallel-tangent constraint between the two interpolating splines is enforced at each knot.

Spline knots are obtained as subsampled lists Q_A and Q_B of n coupled edge points $(x_{A,i}, y_{A,i})$ and $(x_{B,i}, y_{B,i})$. The sampling period is chosen as the radius of the smallest vessel bend (fastest turn), expressed in pixel, that we want to detect by interpolating edge points. Naming y_A the interpolating spline for one vessel border and y_B for the other, the two splines equations for intervals $[x_{A,i}, x_{A,i+1}]$ and $[x_{B,i}, x_{B,i+1}]$ can be written using the general cubic function. The parallelism constraint is enforced at the right end of each pair of coupled intervals $[x_{A,i}, x_{A,i+1}]$ and $[x_{B,i}, x_{B,i+1}]$: the slopes of the tangents to the splines at $y_A(x_{A,i+1})$ and $y_B(x_{B,i+1})$ must be equal. Thereby, the following overconstrained system is obtained:

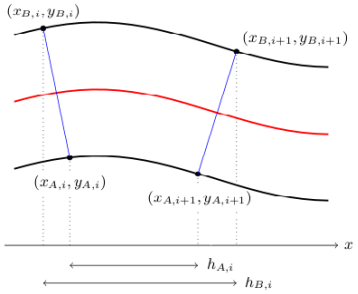

Fig. 4. Spline interpolation of two pair of points enforcing the parallel-tangent constraint.

$$\begin{cases} y_A = a_i(x - x_{A,i})^3 + b_i(x - x_{A,i})^2 + c_i(x - x_{A,i}) + d_i \\ y_B = \alpha_i(x - x_{B,i})^3 + \beta_i(x - x_{B,i})^2 + \gamma_i(x - x_{B,i}) + \delta_i \\ y'_A(x_{A,i+1}) = y'_B(x_{B,i+1}) \end{cases} \tag{1}$$

The last equation in the system leads to:

$$3a_i h_{A,i}^2 + 2b_i h_{A,i} + c_i = 3\alpha_i h_{B,i}^2 + 2\beta_i h_{B,i} + \gamma_i, \tag{2}$$

where $h_{A,i} = x_{A,i+1} - x_{A,i}$, $h_{B,i} = x_{B,i+1} - x_{B,i}$ and coefficients $a_i, b_i, c_i, \alpha_i, \beta_i, \gamma_i$ can be substituted using standard formulae for spline coefficients. Naming $S_{A,i} = y''_A(x_{A,i})$ and $S_{B,i} = y''_B(x_{B,i})$ the second derivative of the function, after some simplifications, the previous equation becomes:

$$\begin{aligned} \frac{1}{3}S_{A,i+1}h_{A,i} + \frac{1}{6}S_{A,i}h_{A,i} - \frac{1}{3}S_{B,i+1}h_{B,i} - \frac{1}{6}S_{B,i}h_{B,i} = \\ = f_B[x_{B,i}, x_{B,i+1}] - f_A[x_{A,i}, x_{A,i+1}] \end{aligned} \tag{3}$$

where $f_A[x_{A,i}, x_{A,i+1}] = \dfrac{y_{A,i+1} - y_{A,i}}{h_{A,i}}$, $f_B[x_{B,i}, x_{B,i+1}] = \dfrac{y_{B,i+1} - y_{B,i}}{h_{B,i}}$ and $i = 0, \ldots, n-1$.

Using the S governing equation for both contours and the parallel-tangent constraint, the system can be written in matrix form, $A\boldsymbol{x} = \boldsymbol{b}$, where:

$$\boldsymbol{x} = \begin{bmatrix} S_{A,1} \\ S_{A,2} \\ \vdots \\ S_{A,n-1} \\ S_{B,1} \\ S_{B,2} \\ \vdots \\ S_{B,n-1} \end{bmatrix} \quad \boldsymbol{b} = \begin{bmatrix} 6(f_A[x_1, x_2] - f_A[x_0, x_1]) \\ \vdots \\ 6(f_A[x_{n-1}, x_n] - f_A[x_{n-2}, x_{n-1}]) \\ 6(f_B[x_1, x_2] - f_B[x_0, x_1]) \\ \vdots \\ 6(f_B[x_{n-1}, x_n] - f_B[x_{n-2}, x_{n-1}]) \\ f_B[x_0, x_1] - f_A[x_0, x_1] \\ \vdots \\ f_B[x_{n-1}, x_n] - f_A[x_{n-1}, x_n] \end{bmatrix}$$

$$A = \left[\begin{array}{c|c} M_1 & 0 \\ \hline 0 & M_2 \\ \hline M_3 & M_4 \end{array}\right] \qquad M_1 = \begin{bmatrix} 2(h_{A,0}+h_{A,1}) & h_{A,1} & 0 & 0 & \dots & 0 \\ h_{A,1} & 2(h_{A,1}+h_{A,2}) & h_{A,2} & 0 & \dots & 0 \\ \vdots & & \ddots & & & \\ 0 & 0 & \dots & h_{A,n-2} & 2(h_{A,n-2}+h_{A,n-1}) & \end{bmatrix}$$

$$M_2 = \begin{bmatrix} 2(h_{B,0}+h_{B,1}) & h_{B,1} & 0 & 0 & \dots & 0 \\ h_{B,1} & 2(h_{B,1}+h_{B,2}) & h_{B,2} & 0 & \dots & 0 \\ \vdots & & \ddots & & & \\ 0 & 0 & \dots & h_{A,n-2} & 2(h_{B,n-2}+h_{B,n-1}) & \end{bmatrix}$$

$$M_3 = \begin{bmatrix} \frac{1}{3}h_{A,0} & 0 & 0 & \dots & 0 \\ \frac{1}{6}h_{A,1} & \frac{1}{3}h_{A,1} & 0 & \dots & 0 \\ \vdots & & \ddots & \ddots & \vdots \\ & & & & \frac{1}{3}h_{A,n-2} \\ 0 & 0 & \dots & 0 & \frac{1}{6}h_{A,n-1} \end{bmatrix} \qquad M_4 = \begin{bmatrix} -\frac{1}{3}h_{B,0} & 0 & 0 & \dots & 0 \\ -\frac{1}{6}h_{B,1} & -\frac{1}{3}h_{B,1} & 0 & \dots & 0 \\ \vdots & & \ddots & \ddots & \vdots \\ & & & & -\frac{1}{3}h_{B,n-2} \\ 0 & 0 & \dots & 0 & -\frac{1}{6}h_{B,n-1} \end{bmatrix}$$

This system is overconstrained by the parallelism constraint at knots, and can be solved by least squares, e.g. by SVD. Having values $S_{A,i}$ and $S_{B,i}$ from the solution $\hat{\boldsymbol{x}}$, the coefficients $a_i, b_i, c_i, d_i, \alpha_i, \beta_i, \gamma_i$ and δ_i are given by standard spline formulae.

2.5. Width estimation

The vessel width w_j at point C_j lying on the spline-smoothed centreline is estimated computing the Euclidean distance between points D_j and E_j: these are the points belonging to the two refined contours and lying on segment d_j, orthogonal to centreline at C_j.

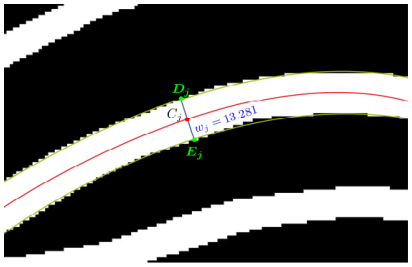

Fig. 5. Vessel width at C_j estimated as the Euclidean distance w_j between D_j and E_j.

3. EXPERIMENTAL RESULTS

The width measurement performance is evaluated using the publicly available REVIEW database [10]. This database comprises four image sets offering a representative spectrum of vessel appearance in fundus images: high-resolution (HRIS dataset), central light reflex (CLRIS dataset), vascular diseases (VDIS dataset) and kickpoints (KPIS dataset). All the images were assessed by three different experts (observers) that manually marked vessel edge points; the average of these three diameter measurements is considered as the ground truth width. REVIEW contains a total of 5066 manually marked profiles. Naming O_1, O_2 and O_3 the three observers, the reference standard vessel diameter at ith location is the mean ψ_i of width measurements from O_1, O_2 and O_3. For comparison of different algorithms, the error χ_i is defined as $\chi_i = w_i - \psi_i$ where w_i is the width at ith location estimated by the algorithm under examination. The standard deviation σ_χ of the error is used to evaluate algorithm performance, as it is deemed more important to produce results that are precise than accurate [5]. The error mean μ_χ and the standard deviation σ and μ of the measurements w are also reported. A further useful parameter for performance evaluation is the success rate (SR), i.e. the number of meaningful measurements returned by the algorithm over the total number of profile reported in the database.

In order to compare ψ_i with our estimate, the following procedure is applied: for each pair of ground truth vessel edge co-ordinates $(x_{A,O}, y_{A,O})$ and $(x_{B,O}, y_{B,O})$ in REVIEW, the reference standard centreline point $C_O(x_C, y_C)$ is computed, where $x_C = \dfrac{x_{A,O}+x_{B,O}}{2}$ and $y_C = \dfrac{y_{A,O}+y_{B,O}}{2}$. The method described in Section 2.5 to find w_i is applied to point C_j, which is the closest to C_O lying on the spline-smoothed centreline.

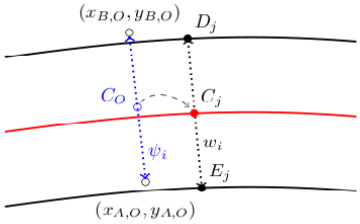

Fig. 6. Ground truth centreline point C_O and the closest point C_j lying on the spline-smoothed centreline.

Table 1 reports the performance of our method and its comparison with algorithms reported in the literature: Extraction of Segment Profiles (ESP) procedure [6] and Xu's graph-based method [7]. The accuracy achieved with simple double-spline fit with parallelism constraint at knots is comparable accuracy to that of specialized, sophisticated width estimation algorithm. The proposed method has a performance comparable to the observers in HRIS dataset: $\sigma_\chi = 0.760$ pixels (2.75 times the mean of observers' σ_χ). Nevertheless, Xu's graph-based method and ESP algorithm perform slightly better. On the contrary, in CLRIS dataset, the spline-based

Table 1. Performance comparison of the width measurement methods on the REVIEW database

Method	Measurement		Error		SR %	Measurement		Error		SR %
	μ	σ	μ_χ	σ_χ		μ	σ	μ_χ	σ_χ	
	HRIS					CLRIS				
First observer: O_1	4.12	1.25	-0.23	0.288	100	13.19	4.01	-0.61	0.567	100
Second observer: O_2	4.35	1.35	0.002	0.256	100	13.69	4.22	-0.11	0.698	100
Third observer: O_3	4.58	1.26	0.23	0.285	100	14.52	4.26	0.72	0.566	100
Ground truth: O	4.35	1.26	-	-	100	13.80	4.12	-	-	100
ESP [6]	4.63	-	0.28	0.420	99.7	15.7	-	-1.90	1.469	93.0
Graph [7]	4.56	1.30	0.21	0.567	100	14.05	4.47	0.08	1.78	94.1
Proposed method	**3.93**	**1.40**	**-0.42**	**0.760**	**95.7**	**13.81**	**3.68**	**-0.16**	**1.229**	**90.2**
	VDIS					KPIS				
First observer: O_1	8.50	2.54	-0.35	0.543	100	7.97	0.47	0.45	0.233	100
Second observer: O_2	8.91	2.69	0.06	0.621	100	7.60	0.42	0.08	0.213	100
Third observer: O_3	9.15	2.67	0.30	0.669	100	7.00	0.52	-0.53	0.234	100
Ground truth: O	8.85	2.57	-	-	100	7.52	0.42	-	-	100
ESP [6]	8.80	-	-0.05	0.766	99.6	6.56	-	-0.96	0.328	100
Graph [7]	8.35	3.00	-0.53	1.43	96.0	6.38	0.59	-1.14	0.67	99.4
Proposed method	**8.17**	**2.82**	**-0.79**	**1.381**	**92.1**	**6.06**	**0.28**	**-1.32**	**0.319**	**93.9**

method reports the best accuracy, despite the central light reflex. Its success rate is yet lower than ESP and Xu's algorithms. On the noisy VDIS dataset the width measurement by our spline-based contours refinement reports the second best performance after ESP. Finally, in KPIS dataset the spline-based method reports again the best performance, even though it scores a SR slightly lower that other algorithms.

Processing times obtained using a MATLAB implementation of the spline-based algorithm range from 2.09 seconds for vessel of 57 pixels to 7.15 for vessels of 362 pixels. Tests ran on an Intel(R) Core(TM)2 Duo CPU (2.26 GHz) with 3GB RAM memory.

4. CONCLUSION AND FUTURE WORK

We proposed a novel algorithm for refining vessel boundaries in retinal binary vessel maps. The spline-based algorithm provides an improved version of the input binary image, in which vessel contours are smoothed. The contours refinement method proposed improves vessel width estimations since vascular boundaries are smoothed and the typical indentation of binary edges is removed. Thus, multiple diameter measurements along the same vessel do not present a high standard deviation any longer. The width estimations achieved with simple double-spline fit with parallelism constraint at knots have accuracy comparable to that of specialized, sophisticated algorithms. The algorithm is general enough to be applied to any kind of retinal binary mask, even to black-and-white images not representing a full eye fundus.

One limitation of this approach is that its diameter evaluation performance strictly relies on the accuracy of the input binary image. The integration of the spline-based algorithm with more accurate vessel segmentation procedures may lead to an improved performance in width measurements.

5. REFERENCES

[1] J.V.B. Soares, J.J.G. Leandro, R.M. Cesar, H.F. Jelinek, and M.J. Cree, "Retinal vessel segmentation using the 2-D Gabor wavelet and supervised classification," *IEEE Trans. on Med. Im.*, vol. 25, pp. 1214–1222, Sept. 2006.

[2] C. A. Lupascu, D. Tegolo, and E. Trucco, "FABC: retinal vessel segmentation using AdaBoost," *IEEE Trans. on Inf. Tech. in Biom.*, vol. 14, no. 5, pp. 1267–1274, Sept. 2010.

[3] B.S.Y. Lam, Yongsheng Gao, and A.W.-C. Liew, "General retinal vessel segmentation using regularization-based multiconcavity modeling," *IEEE Trans. on Med. Im.*, vol. 29, no. 7, pp. 1369 –1381, July 2010.

[4] M.M. Fraz, P. Remagnino, A. Hoppe, B. Uyyanonvara, A.R. Rudnicka, C.G. Owen, and S.A. Barman, "Blood vessel segmentation methodologies in retinal images a survey," *Comp. Met. Prog. Bio.*, vol. 108, no. 1, pp. 407–433, Oct. 2012.

[5] J. Lowell, A. Hunter, D. Steel, A. Basu, R. Ryder, and R.L. Kennedy, "Measurement of retinal vessel widths from fundus images based on 2-D modeling," *IEEE Trans. on Med. Im.*, vol. 23, no. 10, pp. 1196–1204, Oct. 2004.

[6] B. Al-Diri, A. Hunter, and D. Steel, "An active contour model for segmenting and measuring retinal vessels," *IEEE Trans. on Med. Im.*, vol. 28, pp. 1488–1497, Sept. 2009.

[7] X. Xu, M. Niemeijer, Q. Song, M. Sonka, M. K. Garvin, J. M. Reinhardt, and M. D. Abramoff, "Vessel boundary delineation on fundus images using graph-based approach," *IEEE Trans. on Med. Im.*, vol. 30, no. 6, pp. 1184–1191, 2011.

[8] D. Fiorin, E. Poletti, E. Grisan, and A. Ruggeri, "Fast adaptive axis-based segmentation of retinal vessels through matched filters," in *IFMBE Proc.*, 2009, vol. 25/11, pp. 145–148.

[9] S. Chaudhuri, S. Chatterjee, N. Katz, M. Nelson, and M. Goldbaum, "Detection of blood vessels in retinal images using two-dimensional matched filters," *IEEE Trans. on Med. Im.*, vol. 8, no. 3, pp. 263 –269, Sept. 1989.

[10] B. Al-Diri, A. Hunter, D. Steel, M. Habib, T. Hudaib, and S. Berry, "REVIEW-A reference data set for retinal vessel profiles," in *Int. Conf. of IEEE-EMBS*, 2008, pp. 2262–2265.